

## Polymer Microbubbles As Diagnostic and Therapeutic Gas Delivery Device

Francesca Cavaliere,<sup>†</sup> Ivana Finelli,<sup>†</sup> Mariarosaria Tortora,<sup>†</sup> Pamela Mozetic,<sup>†</sup> Ester Chiessi,<sup>†</sup> Francesca Polizio,<sup>†</sup> Torkel B. Brismar,<sup>‡</sup> and Gaio Paradossi<sup>\*,†</sup>

Dipartimento di Scienze e Tecnologie Chimiche, Università di Roma Tor Vergata, Via della Ricerca Scientifica, 00133 Rome, Italy, and Department of Radiology, Karolinska Institutet, Stockholm, Sweden

Received December 29, 2007. Revised Manuscript Received February 14, 2008

Nitric oxide plays a central role in controlling arterial thrombosis and in cardiovascular diseases by inhibiting the platelet aggregation process. This process is regulated by giving a deactivating signal for the protein membrane integrins, the major platelet adhesion receptors. The localized production of NO, naturally occurring in arterial vessels, is carried out by the NO synthase enzymatic system. Inhibition of platelets aggregation in the coagulation cascade process is due to the antagonist action of NO toward integrin-fibrinogen induced platelet adhesion. However, sometimes the natural supply of NO is not sufficient to prevent clotting. The design of devices for suitable transport and delivery of NO is therefore important. We are developing a new concept of drug delivery in which NO release can be performed by means of polymer shelled microbubbles. The NO release can theoretically be concentrated in vessels with acute thrombosis by bursting of the microparticles upon insonification. This feature is linked to the structural and mechanical properties of the particles shell and it would make minimally invasive local therapy of acute vascular disease feasible. In this paper, we present a study on some new structural and mechanical features of this microdevice supporting its NO loading capacity and in vitro efficacy in preventing the formation of a clot by releasing NO.

### Introduction

Diseases with a high impact for modern society, such as cardiovascular disease and cancer, might in the near future be treated using micro/nanodesigned diagnostic and therapeutic devices. Ideally, these devices can be used for both early diagnosis and treatment by local release.

Ultrasound contrast agents are examples of microimaging devices that already are in medical use. They consist of micrometer-sized bubbles made of a lipidic shell with a core containing a stabilizing gas,<sup>1</sup> which are injected in the bloodstream. If the bubbles providing the contrast effect in the ultrasound imaging methodologies can be loaded with drugs, local release and local noninvasive therapy will be possible.<sup>2</sup> To further improve their diagnostic and therapeutic features, they should ideally also be able to target the tissue by chemical binding or affinity.<sup>3</sup>

In recent years, the formulation and the characteristics of air-filled and polymer shelled microballoons originating from

a cross-linking reaction of poly(vinyl alcohol), PVA, at the air/water interface has been described.<sup>4</sup> These bubbles have successfully been decorated with several molecules on the external surface,<sup>5</sup> enabling attachment of ligands to the surface of the microbubbles.<sup>6</sup>

Microbubbles are well-suited for delivery of biologically active gases. Among these, nitric oxide, NO, is an important factor in many relevant bioprocesses.<sup>7</sup> The different physiological roles and therapeutic properties of this gas span from endothelium regeneration<sup>8,9</sup> to regulation of the cardiovascular system,<sup>10</sup> to antithrombotic activity.<sup>11</sup>

In this study, we present new features of PVA-based microbubbles concerning the loading with NO. The main structural requirement for using microbubbles as ultrasound contrast agent are dictated by their injectability in the circulatory system. Therefore, their size should not overcome

\* Corresponding author. E-mail: paradossi@stc.uniroma2.it. Fax: 39 06 7259 4328.

<sup>†</sup> Università di Roma Tor Vergata.

<sup>‡</sup> Karolinska Institutet.

- (1) Schutt, E. G.; Klein, D. H.; Mattrey, R. M.; Riess, J. G. *Angew. Chem., Int. Ed.* **2003**, *42*, 3218.
- (2) Unger, E. C.; Matsunaga, T. O.; McCreery, T.; Schumann, P.; Sweitzer, R.; Quigley, R. *Eur. J. Radiol.* **2002**, *42*, 160.
- (3) Klibanov, A. L. *Adv. Drug Delivery Rev.* **1999**, *37*, 139.

(4) Cavaliere, F.; El Hamassi, A.; Chiessi, E.; Paradossi, G. *Langmuir* **2005**, *21*, 8758.

(5) Cavaliere, F.; El Hamassi, A.; Chiessi, E.; Paradossi, G.; Villa, R.; Zaffaroni, N. *Biomacromolecules* **2006**, *7*, 604.

(6) Klibanov, A. L. *Bioconjugate Chem.* **2005**, *16*, 9.

(7) Nathan, C. *FASEB J.* **1992**, *6*, 3051–3064.

(8) Ignarro, L. J. *FASEB J.* **1989**, *3*, 31.

(9) Ignarro, L. J.; Buga, G. M.; Wood, K. S.; Byrns, R. E.; Chaudhuri, G. *Proc. Natl. Acad. Sci. U.S.A.* **1987**, *84*, 9265.

(10) Palmer, R. M. J.; Ferridge, A. G.; Moncada, S. *Nature* **1987**, *327*, 524.

(11) Jackson, S. P.; Schoenwaelder, S. M. *Nat. Rev.: Drug Discovery* **2003**, *2*, 1.

the lumen of the capillaries, i.e., they should not be bigger than a red blood cell and they should have a limited polydispersity. Fabrication of PVA-based microbubbles can be performed in different pH and temperature conditions with a limited influence on their size, diameter distribution, and shell thickness. The bubbles presented in this study, MBpH5RT, were prepared at pH 5 at room temperature. The details of the procedure of fabrication of the bubbles has been published elsewhere.<sup>4,12</sup>

The aim of this paper is to demonstrate that PVA-shelled microbubbles can be loaded with NO and that the colloidal stability of these NO loaded bubbles can in principle enable local delivery when the particle shell has a suitable flexibility. This feature has been probed by converting the PVA shelled microbubbles into microcapsules and it opens a new perspective for the use of this device for local delivery of drugs other than gases.

### Experimental Section

**Materials.** Poly(vinyl alcohol) (PVA) was a Sigma product (Germany) with number average molecular weight ( $M_n$ ) of 35 000. Sodium poly(styrenesulfonate, sodium salt) (NaPSS)  $M_n$  70 000, Rhodamine B isothiocyanate (RBITC), and fluorescein isothiocyanate isomer I (FITC) were Fluka products (Germany). Fluorescein isothiocyanate-labeled dextrans (FITC-dextran) with molecular weights of 4000, 10 000, 20 000, and 70 000 and labeling density of 0.004 mol of FITC/mol of glucose were also supplied by Sigma. Dimethyl sulfoxide (DMSO), sodium periodate, and inorganic acids used for microbubbles preparation were RPE products from Carlo Erba (Italy).

Platelets were purchased from Helena Bioscience Europe. Epinephrine,  $\text{CaCl}_2$ , glutathione, sodium dithionite, fibrinogen, and thrombin were Sigma products used without further purification. Double distilled water with resistivity of 12.8  $\text{M}\Omega$  cm (MilliQ water) was used throughout this study.

**Methods. Microbubble Fabrication.** The fabrication of PVA-based microbubbles has been reported recently.<sup>4</sup> In summary, 2 g of PVA were dissolved in 100 mL of MilliQ water and oxidized by sodium periodate during high shear stirring (8000 RPM for 3 h) with an Ultra Turrax (IKA, Germany) at room temperature.

**Confocal Laser Scanning Microscopy (CLSM).** FITC and RBITC were used for fluorescent labeling of microbubbles, microcapsules, and fibrinogen. Fluorescent dyes were added to the microbubble suspension at a typical concentration of 10 mM. The mixture was then stirred for 2 h. Floating particles were washed by resuspending in MilliQ water several times. Fibrinogen was labeled with FITC in 0.1 M carbonate buffer at pH 8.5 and FITC/protein weight ratio of 1.20. Confocal images were collected by a confocal laser scanning microscope, Nikon PCM 2000 (Nikon Instruments): a compact laser scanning microscope based on a galvanometer point-scanning mechanism, a single pinhole optical path and a multiexcitation module equipped with Spectra Physics Ar-ion laser (488 nm) and He-Ne laser (543.5 nm) sources. A 60 $\times$ /1.4 oil immersion objective was used for the observations.

**Freeze-Fracture Electron Microscopy.** The analysis was carried out by NanoAnalytical Laboratory, San Francisco, CA, on a microbubble sample prepared at room temperature at pH 5 in  $\text{H}_2\text{O}$ . The sample was quenched using sandwich technique and liquid

nitrogen-cooled propane. Using this technique, a cooling rate of 10 000 K/s is reached, avoiding ice crystal formation and artifacts possibly caused by the cryofixation process. The cryofixed sample was stored in liquid nitrogen for less than 2 h before processing. The fracturing process was carried out in a JEOL JED-9000 freeze-etching equipment (JEOL, Japan) and the exposed fracture planes were shadowed with platinum for 30 s in an angle of 25–35° and with carbon for 35 s (2kV/60–70 mA, 10–5 Torr). The replicas produced in this way were cleaned with concentrated, fuming  $\text{HNO}_3$  for 24 h, followed by repeating agitation with fresh chloroform/methanol (1:1 by vol.) at least 5 times. The replicas were then examined using a JEOL 100 CX (JEOL, Japan) or Philips CM 10 (Philips, The Netherlands) electron microscope.<sup>13</sup>

**EPR of NO Loaded Microbubbles and NO Release.** A water suspension of microbubbles was freeze-dried and the resulting powder (typically 30 mg) was placed in a stainless steel reactor with a volume of 250 mL. The vessel, connected to an NO tank by stainless steels luer-lock connections, was pressurized to 1.5 bar and left in this condition for 3 h. Freeze-dried NO loaded microbubbles were then suspended in a 1 mM myoglobin and sodium dithionite to ensure reducing conditions. X band EPR spectra were recorded on a EMX Bruker spectrometer (Bruker, Germany) operating at  $T = 100$  K at 0.5 mT field modulation.<sup>14</sup>

**In vitro Anticlotting Effect of NO Loaded Microbubbles.** A blank experiment was performed by mixing platelets and unloaded microbubbles in the clotting medium containing epinephrine,  $\text{CaCl}_2$ , glutathione, sodium dithionite, fibrinogen, and thrombin dispersed in PBS. Platelets and microbubbles were tagged with FITC for CLSM analysis.

For the in vitro tests on the anticlotting activity of NO loaded microbubbles, the previous experiment was carried out (A) immediately after the opening of the vessel used for the loading operation, (B) after 1 h, and (C) after 3 h. Pictures were taken after 1 h from the mixing.

**Conversion of Microbubbles to Microcapsules and Osmotic Stress Experiments.** Concentrated microbubble dispersion was equilibrated in DMSO for 2 days. DMSO was then replaced with water by exhaustive dialysis. The conversion to capsules was evidenced by the presence of particles at the bottom of the dialysis chamber. The size of the pores in the microcapsule surface was studied by CLSM evaluation of the penetration or exclusion of FITC-labeled dextrans with monodispersed molecular weight distributions.

Osmotic stress experiments were carried out by equilibrating the water containing PVA microcapsules against aqueous solutions at increasing concentrations of polyelectrolyte sodium poly(styrene sulfonate), NaPSS. To avoid any permeation of the polyelectrolyte through the microbubble shells, we used a molecular weight of 70 000 Daltons. The morphology of the microparticles at different external polyelectrolyte concentrations was evaluated by CLSM.

**Echographic Imaging.** Echographic images were recorded with a standard medical instrument (Acuson Sequoia, Siemens, Germany).

### Results and Discussion

**Microbubble Characterization.** In this study, microbubbles prepared at pH 5 and at room temperature, MBpH5RT, according to the procedure already outlined,<sup>4,5,12</sup> are characterized by CLSM and freeze-fractured electron microscopy. MBpH5RT bubbles have an average external diameter by confocal microscopy of 4.6  $\mu\text{m}$  with a standard deviation of 0.4  $\mu\text{m}$ . Freeze-fracture electron microscopy analysis with

(12) Cavalieri, F.; El Hamassi, A.; Chiessi, E.; Paradossi, G.; Villa, R.; Zaffaroni, N. *Macromol. Symp.* **2006**, *234*, 94.

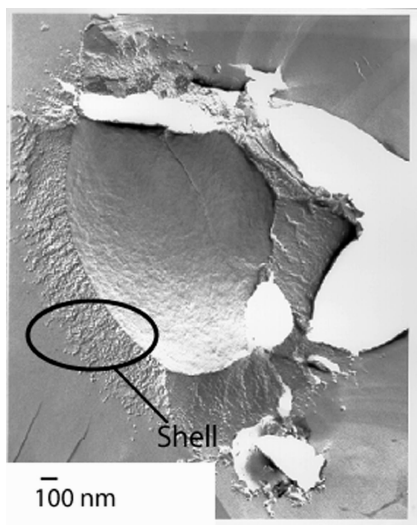


**Figure 1.** Electron micrograph of freeze-fractured microbubble fabricated at pH 5 at room temperature showing a shell thickness of  $0.4 \mu\text{m}$  with a microstructure consisting of PVA microfibrils.

a typical resolution of 2 nm allows the evaluation of a shell thickness of  $0.4 \mu\text{m}$  and a morphology consisting of a nonuniform radial density of the polymer shell. As evidenced in the circled area of the cross section of a freeze-dried bubble, Figure 1, there is an outer region characterized by loosely arranged PVA fibrils and an inner region where the polymer material is organized in a more compact fashion. In the outer domains of the shell, PVA fibrils protrude radially toward the outside.

The colloidal stability of microbubbles<sup>4</sup> may be attributed to the presence of polymer chains extending into the solution and forming the “hairy” surface shown in Figure 1.

The influence of some reaction parameters as pH and temperature has been investigated in preliminary work. As highlighted in previous papers,<sup>4,5</sup> the shell formation is the result of a cross-linking reaction at the water/air interface between the aldehyde chain terminals of oxidized PVA and the hydroxyl groups of the polymer backbone. This condensation reaction is catalyzed at low pH's. Comparing the bubbles formed at pH 5 with the ones obtained at pH 2, it can be inferred that the latter show an increased shelf life and robustness, and a decreased shell reactivity toward coupling with amino-compounds, indicating the presence of a smaller amount of unreacted aldehydes as expected for acid catalyzed reactions. Temperature is a parameter mostly influencing the gas solubility and therefore bubble dimensions. Nitrogen solubility in water is increased at lower temperature, promoting the formation of smaller size bubbles.

**NO Loading of Microbubbles.** NO loading of microbubbles is carried out by exposing freeze-dried microbubbles in a stainless steel vessel to NO at 1.5 bar for 2 h. Because of the lability of this molecule, the detection of NO in an aqueous dispersion of microbubble is performed by binding the molecule with myoglobin (Mb). The electron paramagnetic resonance spectroscopy, EPR, of the NO–Mb complex is well-characterized in the literature and can be regarded as a fingerprint of the loading of NO on microbubbles. The EPR spectrum at 100 K of NO released by the bubbles in an aqueous solution of myoglobin is indicative of the six

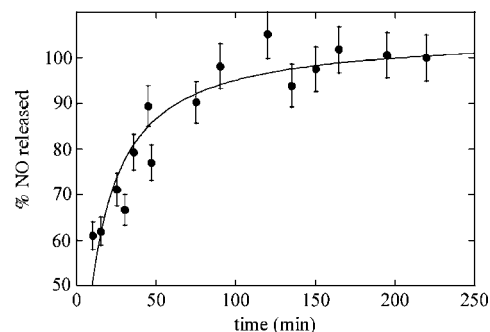


**Figure 2.** Release of NO by microbubbles measured as nitrites by Griess assay.

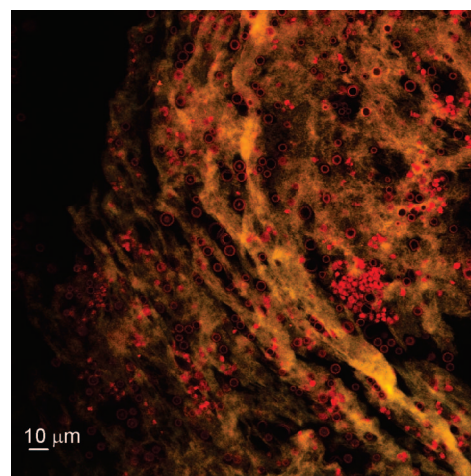


**Figure 3.** CLSM image of a clot formed in vitro with RBITC tagged platelets (red dots) and entrapped unloaded microbubbles (red rings).

coordinate nitrosyl-heme complex with the characteristic  $g_1 = 2.08$ ,  $g_2 = 2.01$ , and  $g_3 = 1.98$  values.<sup>15</sup> Moreover, the EPR spectrum shows that NO molecules are stored in the bubbles as such without undergoing any chemical transformation with the polymeric moiety.

The NO release is evaluated indirectly by Griess colorimetric assay of nitrites and nitrates generated from the NO oxidation. The initial time lag in Figure 2 refers to the time lapse occurring from the opening of the container to the transfer of the NO loaded microbubbles into PBS solution.

The initial release burst of 60%, shown in Figure 2, is due to the oxidation of NO during this initial time lag. The remaining 40% of the total NO loaded in the microbubbles is released in PBS in about 2 h, a suitable time window for routine echographic manipulations. The average NO content per milligram of microbubbles is  $3.6 \mu\text{mol}$ , corresponding to about 1% of the NO present in the reaction vessel during the loading procedure.

To test the ant clotting effect of NO loaded microbubbles, we carried out in vitro experiments by monitoring clot formation by CLSM in the presence of unloaded and NO loaded microbubbles. Figure 3 shows a blank experiment where the clot is visualized by fibrinogen tagged with

(13) Papahadjopoulos-Sternberg, B.; Ackrell, J. *Microsc. Microanal.* **2006**, *12*, 1126.

(14) Polizio, F.; De Sanctis, G.; Ascenzi, P.; Coletta, M. *J. Biol. Inorg. Chem.* **1998**, *3*, 458.

(15) Archer, S. *FASEB J.* **1993**, *7*, 349.

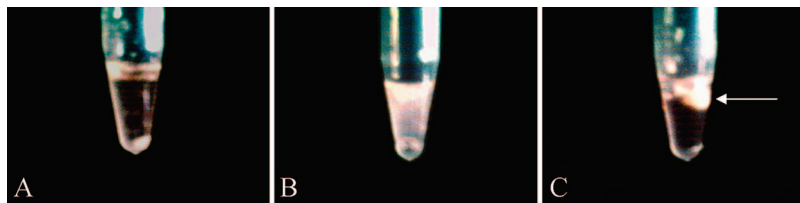


**Figure 4.** (A) Clotting medium in the presence of NO loaded microbubbles used immediately after reaction container opening (time 0 condition); (B) clotting medium in the presence of NO loaded microbubbles after 1 h from the reaction container opening; (C) NO loaded microbubbles after 2 h from the reaction container opening do not prevent the formation of a clot (arrow). Pictures were taken 1 h after microbubble addition to the clotting medium.

fluorescein isothiocyanate, FITC. Platelets and entrapped unloaded microbubbles are labeled with RBITC and detected by CLSM (see Figure 3) as red dots and red rings, respectively.

This experiment indicates that the presence of unloaded microbubbles does not inhibit clot formation. When bubbles are loaded with NO, they inhibited clot formation if used immediately after opening the container (Figure 4A). If bubbles are used 1 h after the opening of the container, some of this ability is lost. In our experiment, the formation of a clot is inhibited, but a stable fibrin gel-like network was achieved (Figure 4B). NO loaded microbubbles left in the atmosphere for 2 h were not able to prevent the formation of clot (Figure 4C).

To the best of our knowledge, this is the first example of an in vitro NO localized delivery device to inhibit clot formation. The use of microbubbles as next-generation ultrasound contrast agent, i.e., for both diagnostic and therapeutic purposes, resides on the shell acoustic behavior. A study on the ultrasound properties of PVA-based microbubbles has been carried out recently.<sup>16</sup> The value of the pressure threshold,  $P_{thr}$ , at which the bubble shells cracked upon insonification has been found within the safety range of mechanical index, MI, recommended for biomedical uses.<sup>17</sup> This parameter is defined as the ratio  $P_{thr}/\sqrt{f}$ , where  $f$  is the ultrasound frequency.

It is noteworthy that the threshold value does not change whether the suspension medium is water or blood. Images of a cylindrical container filled with microbubbles suspended in either water or blood were acquired by means of a commercial medical imaging system at three values of the mechanical index (below, at, and above the MI required to crack the bubbles). Figure 5 illustrates that in all six cases, the microbubbles provided good contrast enhancement.

The mechanical properties of the microbubbles and their responsiveness to ultrasound are affected by the cross-link density and average porosity of the polymer shells. To this respect, an interesting feature of PVA-based microbubbles resides in the possibility to transform them into microcapsules by dispersing the bubbles in dimethyl sulfoxide, DMSO. PVA-based microbubbles are stable in water for months. However, when they are dispersed in DMSO, the empty cavity is filled by the organic phase in a few hours. In fact, DMSO is a good solvent for PVA, and the shell of the microbubbles is expected to swell in this medium. The

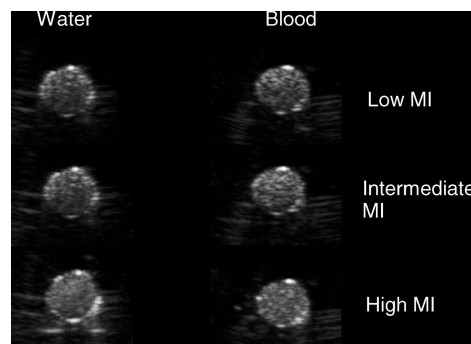


**Figure 5.** Images of MBpH5RT suspended in water (left) and in blood (right) at three values of the mechanical index, MI.

**Table 1. Determination of the Porosity of PVA-Based Microcapsules by Size Exclusion Measurements**

dextran mol wt (g/mol)	hydrodynamic radius (nm)	penetration through MCpH5RT shell
70 000	6.5	no
20 000	3.5	no
10 000	2.7	yes
4000	1.7	yes

consequent increase in the pore size facilitates the permeation of DMSO into the inner cavity, transforming the bubbles into capsules. At this point the encapsulated DMSO can be replaced with other solvents, i.e., water, by dispersing the particles in the new medium. This feature opens the perspective to the use of PVA-shelled capsules as carrier for water-soluble drugs. CLSM analysis of the microcapsules shows that the conversion of the microbubbles into microcapsules does not affect the average external diameter and shell thickness. As shown in Table 1, the average porosity of the PVA-based microcapsules is about 3 nm (on the basis of the hydrodynamic radii of dextrans reported in the literature).<sup>18</sup>

The conversion of bubbles into capsules offers the opportunity to use osmotic stress for evaluating the shell elasticity. The experiment is carried out by equilibrating the water containing PVA microcapsules against aqueous solutions at increasing concentrations of the polyelectrolyte sodium poly(styrene sulfonate). To avoid any permeation of the polyelectrolyte through the microbubble shells, we used a molecular weight of 70 000 Daltons. The morphology of the microparticles at different external polyelectrolyte concentrations is then evaluated by CLSM as shown in Figure 6a–d.

Once the osmotic pressure in the bulk is larger than in the internal cavity, the hydrostatic pressure difference tends

(16) Pecorari, C.; Grishenkov, D. *J. Acoust. Soc. Am* **2007**, *122*, 2425.

(17) Apfel, R. E.; Holland, C. K. *Ultrasound Med. Biol.* **1991**, *17*, 179.

(18) Gribbon, P.; Hardingam, T. E. *Biophys. J.* **1998**, *75*, 1032.

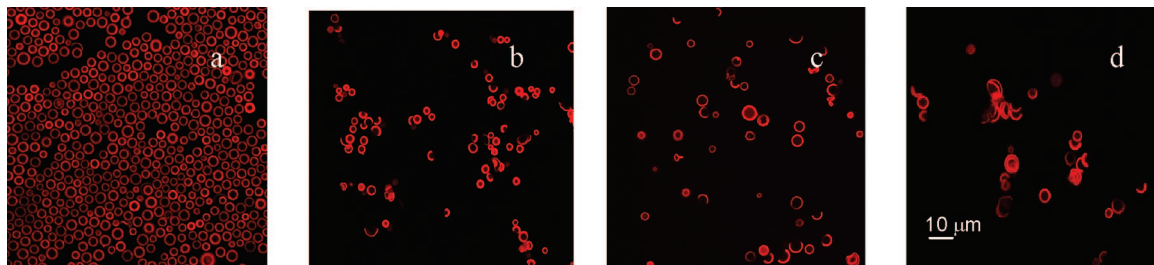


**Figure 6.** NAPSS concentration: 0, 3, 7, and 13% (w/v), a–d, respectively. Scale in (d) is the same for all images.

to deform the microcapsules. Typically, invagination can be noted in the micrographs of RBITC-labeled PVA shells exposed to the highest polyelectrolyte concentration and, at an osmotic pressure greater than 1 MPa, 50% of the capsules are deformed (based on evaluation of sets of 200 microcapsules). Theoretical modeling relating this critical pressure to the mechanical properties of microcapsule shells was developed and applied for the study of microcapsules made by layer-by-layer polyelectrolytes adsorption.<sup>19</sup> In this approach, capsules lose their Euler stability with consequent deformation when the work performed by external pressure is equal to the deformation energy. For this system the Young modulus,  $E$ , is

$$E = \frac{3}{4} \pi_c (R/\delta)^2 \quad (1)$$

where  $\pi_c$  is the critical pressure at the buckling transition, i.e., when half of the sampled microbubbles are deformed,  $R$  is the microbubble radius and  $\delta$  is the shell thickness determined by CLSM. The value of the Young modulus,  $E$ , determined according to eq 1 for the microcapsules under study, is found equal to 4.5 MPa, in good agreement with the values reported for elastomeric films,<sup>20</sup> but much smaller than the value found with the same method for

capsules prepared by layer-by-layer polyelectrolytes deposition.<sup>21</sup>

### Concluding Remarks

The screening of some functional properties of PVA shelled microbubbles for a new concept of multifunctional ultrasound contrast agent provides an encouraging background for further studies. From this work, we find that NO loaded microbubbles are stable and NO cargo molecules do not undergo any chemical variation. The delivery of NO occurs on a time scale compatible with parenteral administration and simultaneous diagnostic use of microbubbles. We have also assessed that in vitro released NO is effective as anticlotting agent, implying the absence of NO<sub>x</sub> oxidation products during the transfer of NO molecules from the bubbles to the integrin receptor site. The dual nature of the particle, i.e., micro(bubbles ↔ capsules), in principle could open the route to the transport of other therapeutic gases and bioactive nongaseous drug molecules to be released by insonification.

**Acknowledgment.** This work was supported by the GEMI foundation (Sweden) and by the EU project S.I.GHT (Contract 033700).

CM703702D

(19) Gao, C.; Leporatti, S.; Moya, S.; Donath, E.; Möhwald, H. *Langmuir* **2001**, *17*, 3491.

(20) *Polymer Handbook*; Brandrup, J., Immergut, E. H., Grulke, E. A., Eds.; Wiley-Interscience: New York, 1999.

(21) Gao, C.; Donath, E.; Moya, S.; Dudnik, V.; Möhwald, H. *Eur. Phys. J.* **2001**, *E 5*, 21.